

# An Interference Removal Technique for Radio Pulsar Searches

R. P. Eatough<sup>1\*</sup>, E. F. Keane<sup>1</sup>, A. G. Lyne<sup>1</sup>

<sup>1</sup> Jodrell Bank Centre for Astrophysics, Alan Turing Building, University of Manchester, Manchester, M13 9PL, United Kingdom.

1 May 2008

## ABSTRACT

Searches for radio pulsars are becoming increasingly difficult because of a rise in impulsive man-made terrestrial radio-frequency interference. Here we present a new technique, zero-DM filtering, which can significantly reduce the effects of such signals in pulsar search data. The technique has already been applied to a small portion of the data from the Parkes multi-beam pulsar survey, resulting in the discovery of four new pulsars, so illustrating its efficacy.

**Key words:** methods: data analysis - pulsars: general - stars: neutron

## 1 INTRODUCTION

Pulsar search data are often corrupted by the presence of impulsive, broadband and sometimes periodic terrestrial radiation. Such *radio frequency interference* (RFI) originates in unshielded electrical equipment which produces discharges, such as automobile ignition systems, electric motors, and fluorescent lighting, as well as discharge from high-voltage power transmission lines. It may also arise naturally from the radio emission generated in lightning discharges. Such RFI can often be very strong and can even enter receiver systems through the far-out sidelobes of the telescope reception pattern. Several methods have been employed to reduce the effects of RFI, such as clipping intense spikes, removing parts of the fluctuation spectrum, and identifying common signals in the different beams of a multi-beam receiver system. These procedures all require carefully tuned algorithms to remove the interference, and at the same time must cause minimal damage to the astronomical data.

RFI signals are mostly broadband but generally do not display the dispersed signature of radio pulsars. Here, we present a simple algorithm which we call ‘zero-DM filtering’ to selectively remove broadband undispersed signals from data prior to the application of normal pulsar search algorithms. The outline of this paper is as follows: following the description of the algorithm in section 2, in section 3 we show that the procedure does indeed remove much of the interference in typical observing situations and in general greatly improves the visibility of celestial dispersed pulses. In section 4 we present four new pulsars discovered in the Parkes multi-beam pulsar survey (PMPS) after applying the new technique. Finally section 5 is a discussion of the benefits and limitations of the procedure.

## 2 ZERO-DM FILTERING

A fundamental characteristic of broadband pulsar signals is the frequency-dependent dispersion of their pulse arrival times as a result of traversing the ionised component of the interstellar medium. Pulses observed at lower frequency arrive later than their higher-frequency counterparts. The delay,  $t$ , at radio frequency  $f$  (MHz) is given by:

$$t = 4150 \left( \frac{\text{DM}}{f^2} \right) \text{ sec}, \quad (1)$$

where DM is the *dispersion measure*, the integrated column density of free electrons along the line of sight, measured in  $\text{cm}^{-3}\text{pc}$  (e.g. Lyne & Smith 2006). Detecting a pulse with a finite bandwidth receiver results in a broadened pulse profile and a corresponding reduction in pulse signal-to-noise ratio. Before any search for pulses can be performed, the data have to be compensated for the effects of a number of trial values of DM. In order to do this, the bandwidth of the receiver is first split into a number of independent frequency channels, which are appropriately sampled to produce a two-dimensional array of samples,  $S(f_i, t_j)$  at frequency  $f_i$  and time  $t_j$ . Appropriate time delays for a given trial DM are then applied to each frequency channel so that any pulses at this DM are aligned in time. The frequency channels are then summed together to produce a time series of dedispersed data,  $x(t)$ .

The zero-DM filter is implemented prior to the dedispersion described above, by simply calculating the mean of all frequency channels in each time sample and subtracting this from each individual frequency channel in the time sample. Hence the adjusted values of the samples,  $S'(f_i, t_j)$  are calculated as:

$$S'(f_i, t_j) = S(f_i, t_j) - \frac{1}{n_{\text{chans}}} \sum_{i=1}^{n_{\text{chans}}} S(f_i, t_j). \quad (2)$$

\* E-mail: ralph.eatough@pulsarastronomy.net

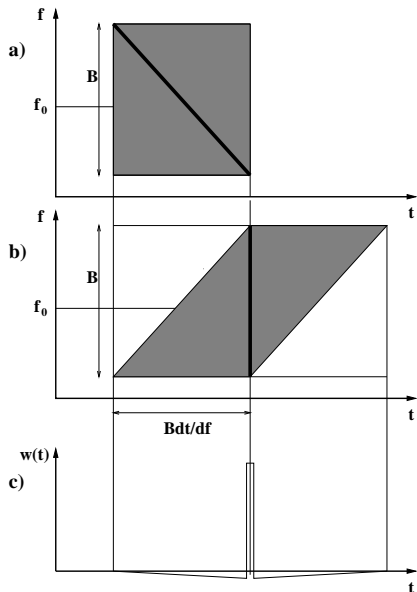


**Figure 1.** The effect of the the zero-DM filter on an idealised narrow linearly-dispersed pulse in the frequency-time domain. The top panel (a) shows the dispersion drift of the pulse  $B dt/df$  over the full bandwidth  $B$  of the receiver. Subtraction of the mean in vertical strips to remove zero-DM signals (Equation 2) leaves the non-pulse area (shaded grey) negative. Panel (b) shows the result of dedispersing the data at the correct value of DM and the lower panel (c) shows the resultant pulse shape after adding all the frequency channels together.

Clearly, any broadband undispersed signal will result in a simultaneous rise across all frequency channels and will be removed by this process. We now investigate the effect of this procedure on dispersed cosmic pulses. Consider an idealised dispersed pulsar signal with very narrow pulses and approximate the dispersion drift across the full receiver bandwidth  $B$  to a linear slope,  $dt/df$ , which is given approximately by:

$$\frac{dt}{df} = -8300 \left( \frac{DM}{f_0^3} \right) \text{ sec/MHz}, \quad (3)$$

where  $f_0$  (MHz) is the central observing frequency. Figure 1a shows such a pulse sweeping through the frequency band of a receiver, traversing the full bandwidth in a time of  $B dt/df$ . After subtraction of the mean in vertical strips as described by Equation 2, the non-pulse grey area in the Figure 1a is negative. Dedispersion then distorts this pattern in the manner shown in Figure 1b, so that adding vertically after the dedispersion then gives the convolving function,  $w(t)$  shown in Figure 1c. Note the negative triangular area which is adjacent to, and equals the area of, the pulse. Thus the zero-DM process results in the dedispersed time series  $x(t)$  being convolved by this function,  $w(t)$ . Of course any real celestial pulse will have a finite width. In Figure 2 we show the effects of the zero-DM filter on idealised box-car pulses of different widths for the PMPS observing system at 1.4 GHz (Manchester et al. 2001). In this case,  $f_0 = 1394$  MHz and  $B=288$  MHz. The pulse width in milliseconds can be calculated by simply multiplying by the DM in  $\text{cm}^{-3}\text{pc}$ . For example, at a DM of  $100 \text{ cm}^{-3}\text{pc}$  the bottom pulse would have a width of 46 ms. The peak amplitude clearly decreases for pulses with larger widths.

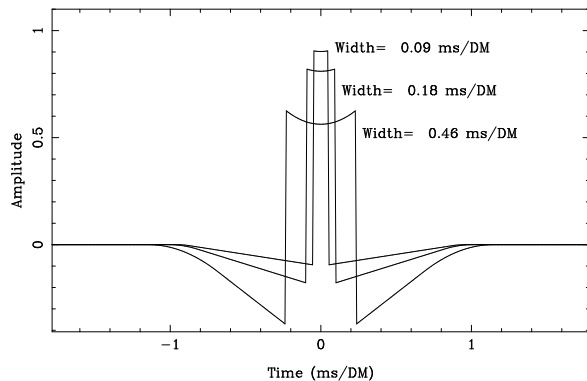


**Figure 2.** The pulse distortion caused by zero-DM filter on idealised box-car pulses of varying width for the PMPS observing system. The time scale should be multiplied by the DM in  $\text{cm}^{-3}\text{pc}$  to give the time in milliseconds.

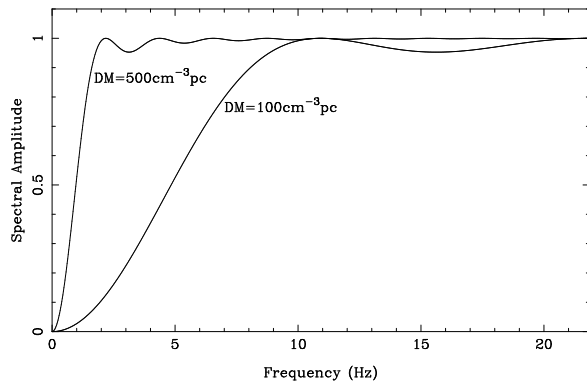


**Figure 3.** Two example effective zero-DM filters for  $DM=500 \text{ cm}^{-3}\text{pc}$  and  $DM=100 \text{ cm}^{-3}\text{pc}$  for the PMPS, showing variation in relative spectral amplitude with the fluctuation frequency.

In the frequency domain, equivalently, the fluctuation spectrum of the dedispersed times series is multiplied by the Fourier transform,  $W(\nu)$ , of  $w(t)$  which can be shown to be of the form:

$$\begin{aligned} W(\nu) &= 1 - \text{sinc}^2\left(\pi B \frac{dt}{df} \nu\right) \\ &= 1 - \text{sinc}^2\left(\frac{8300\pi B DM}{f_0^3} \nu\right), \end{aligned} \quad (4)$$

where  $\nu$  is the fluctuation frequency of the signal. Figure 3 shows the effect of the zero-DM filter on the spectral amplitude of a pulse at two specified DM's for PMPS-style observations. The zero-DM process effectively acts as a high-pass filter on the dispersed pulse. The 'low-frequency cutoff',  $\nu_{\text{cutoff}}$  can be shown using Equation 4 to lie at a fluctuation frequency  $\sim 500/DM$  Hz. Thus for  $DM=100 \text{ cm}^{-3}\text{pc}$ , all frequencies  $< 5$  Hz will be lost. The reduction in amplitude and pulse distortion we see in Figure 2 can be explained by the loss of the low frequency components of the pulse profile.

For a typical pulsar we measure a regular train of narrow pulses, the spectrum of which is a 'picket fence.' The zero-DM filter will cut off all spectral features below  $\nu_{\text{cutoff}}$ . However, normal pulsars with pulse widths a few percent of their pulse period will usually have most of their power in

spectral harmonics at higher frequencies and these will not be affected significantly. Since standard pulsar searches perform harmonic summing (see e.g. Lyne & Smith 2006 or, for a detailed description of pulsar search algorithms, Lorimer & Kramer 2005), the detrimental effect of the zero-DM filter on the final spectral amplitude is reduced. Assuming the pulsar has  $n \sim P/2W$  harmonics of equal amplitude where  $P$  is the pulsar period and  $W$  is the pulse width, the number of harmonics lost below the low-frequency cutoff is given by  $n_{\text{cutoff}} \sim P\nu_{\text{cutoff}}$ , the harmonic summing procedure will increase the spectral signal-to-noise ratio by a factor of approximately  $(n - n_{\text{cutoff}})^{1/2}$ .

The zero-DM process causes a predictable reduction in the amplitudes of low frequencies of the fluctuation spectrum of a dispersed pulsar. It will also reduce the amplitude of any broadband undispersed impulsive signals substantially, but will have little effect upon thermal noise. The signal-to-noise ratio of the pulsar can therefore be optimised by applying an optimum matched filter to the spectrum, which reduces the spectral amplitude where the pulsar signal is known to be small because of the zero-DM filtering. Thus, there is a second step to the filtering process whereby the frequency response of the zero-DM filter is re-applied after each dedispersion trial. In the time domain this is best illustrated by considering a single-pulse search (McLaughlin et al. 2006). Standard single-pulse searches involve convolution of the dedispersed time series  $x(t)$  with box-cars  $b(t)$  of various widths and searching for peaks in  $x(t) * b(t)$ , where  $*$  denotes convolution. In our case, the zero-DM filtered time series is  $x'(t) = x(t) * w(t)$ , so that a standard single-pulse search looks for peaks in  $x'(t) * b(t)$ . As a result of zero-DM filtering the optimal filter is now not a box-car but rather is given by  $b'(t) = b(t) * w(t)$ . We now search for peaks in  $x''(t) = x'(t) * b'(t) = \mathcal{F}^{-1}[X'(\nu) * W(\nu)] * b(t)$  where  $\mathcal{F}$  denotes the Fourier transformation and we have used the commutability of convolution so the convolution can be performed in the frequency domain, which is what is done practice.

### 3 EXAMPLES

The effects of the zero-DM filter have been investigated using simulated PMPS data generated with the *Sigproc-4.2*<sup>1</sup> pulsar analysis software suite. Figure 4a shows simulated data of a 130-ms burst of broadband RFI with  $\text{DM}=0 \text{ cm}^{-3}\text{pc}$  followed by a 20-ms dispersed pulse with  $\text{DM}=150 \text{ cm}^{-3}\text{pc}$  across a 288MHz bandpass centered at 1374 MHz. Figure 4b shows the same data after application of the zero-DM filter. The broadband RFI signal has been completely removed with little effect on the dispersed pulse. Dedispersion at a  $\text{DM}=150 \text{ cm}^{-3}\text{pc}$  and summation in frequency produces the pulse profile shown in Figure 4c. The expected pulse distortion is clearly visible.

We also present examples of the zero-DM filter as applied to observational data from the PMPS in both periodicity and single-pulse searches. All clipping and zapping algorithms used previously for mitigating the effects of RFI (Hobbs et al. 2004) have been omitted. In our periodicity

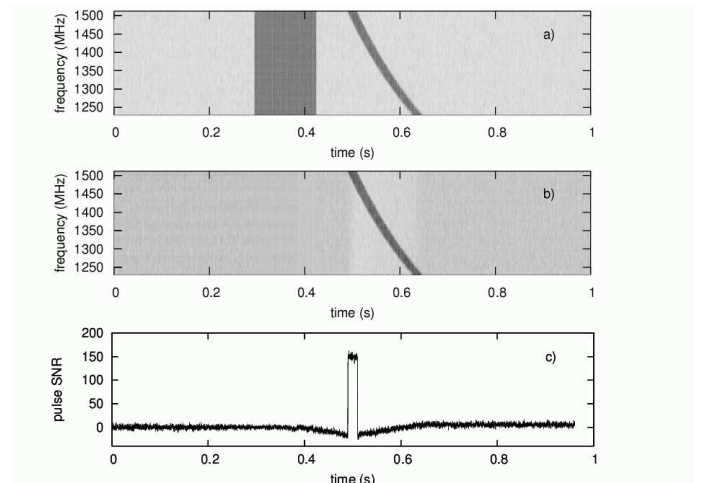


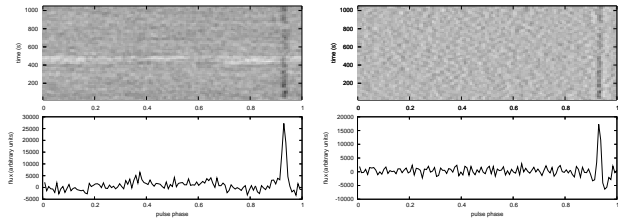
**Figure 4.** The top panel (a) shows a grey plot of simulated data of a 130-ms burst of broadband RFI with  $\text{DM}=0 \text{ cm}^{-3}\text{pc}$  followed by a 20-ms dispersed pulse with  $\text{DM}=150 \text{ cm}^{-3}\text{pc}$  across a 288MHz bandpass centered at 1374 MHz. The middle panel (b) shows the same data after application of the zero-DM filter. Note the negative non-pulse area. In panel (c), the data have been dedispersed for a  $\text{DM}=150 \text{ cm}^{-3}\text{pc}$  and summed in frequency giving the pulse profile.

search examples re-application of the zero-DM filter after each dispersion trial has not been performed because of the additional computational overheads this would impose in our search algorithms (see Section 5 for a further discussion on this subject).

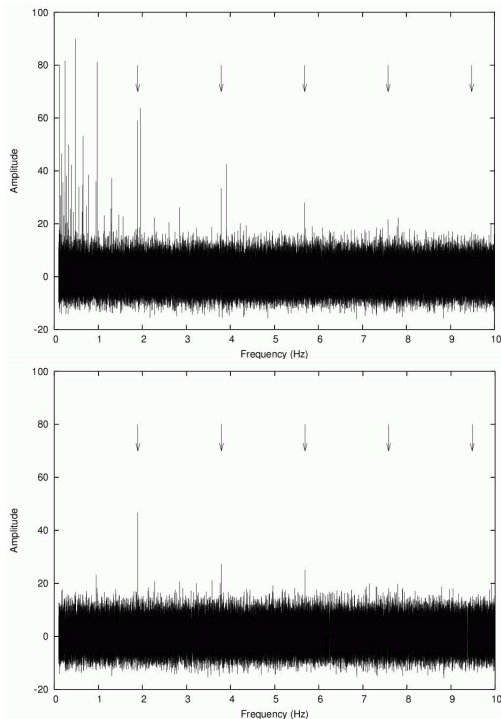
Figure 5 illustrates clearly the effects of the procedure on a 35-minute PMPS observation in the direction of PSR J1842+0257, which has a period of 3.1 seconds and a DM of  $148 \text{ cm}^{-3}\text{pc}$ , so that the zero-DM low-frequency cutoff is at about 3.3 Hz. On the left is the normal search output, while on the right is that with the zero-DM filtering procedure in place. After application of the zero-DM filter the red noise and impulsive interference is almost completely removed, and the expected pulse distortion due to the filtering as shown in Figure 1c and Figure 4c is clear. Remarkably, even with such a long-period pulsar, in which the fundamental and first few harmonics are completely missing, the absence of the interference makes its detection more secure than previously. A number of periodicity searches on PMPS beams containing known pulsars with a range of periods and dispersion measures has been performed. The fluctuation spectra from the periodicity search are much cleaner than before (see Figure 6). The ‘forest’ of RFI signals at low frequency are completely removed by the new technique. The pulsar spectral signal-to-noise ratios behave as expected, but because of the reduction in the number of periodic RFI signals, the pulsars are easier to detect.

Figure 7 shows examples of single-pulse search diagnostic plots from our analysis of the PMPS. Plotted in Figure 7 are the time series for each of the 325 trial DM’s (in the range  $0 - 2200 \text{ cm}^{-3}\text{pc}$ ). Each detected single-pulse event is plotted as a circle with radius proportional to signal-to-noise ratio. The top panel is the result of a standard analysis without zero-DM filtering. The observation contains single pulses

<sup>1</sup> <http://sigproc.sourceforge.net>



**Figure 5.** The effects of the zero-DM filter on folding PMPS data from the 3.1-second pulsar, PSR J1842+0257, which has a DM of  $148 \text{ cm}^{-3}\text{pc}$ . The left-hand panels are the result of using a regular analysis, while the right-hand panels are after application of the zero-DM filter. On each side, at the top are grey plots of 63 temporal sub-integrations folded at the pulse period, covering the full 35-minute survey observation, and at the bottom is a panel showing the full integrated profile. The effect of the filter on the shape of the pulse profile can be clearly seen. The asymmetry of the depressions either side of the pulse arise because the dispersion sweep across the bandpass is not perfectly linear but has a quadratic component, although in most cases the sweep is well approximated by a linear slope. Note that the impulsive RFI present through the majority of the observation is almost completely removed and the baseline wobble in the final profile is much flatter in the filtered case.



**Figure 6.** Fluctuation spectra from a PMPS survey observation in the direction of the 0.53-second pulsar, PSR J1604-4718, which has a DM of  $52 \text{ cm}^{-3}\text{pc}$ . The top panel shows the spectrum without any zero-DM filtering, the bottom panel is the same data after the zero-DM filter has been applied. The arrows indicate the position of the fundamental spin frequency of the pulsar and four subsequent harmonics. Most of the RFI signals are completely removed by the new technique.

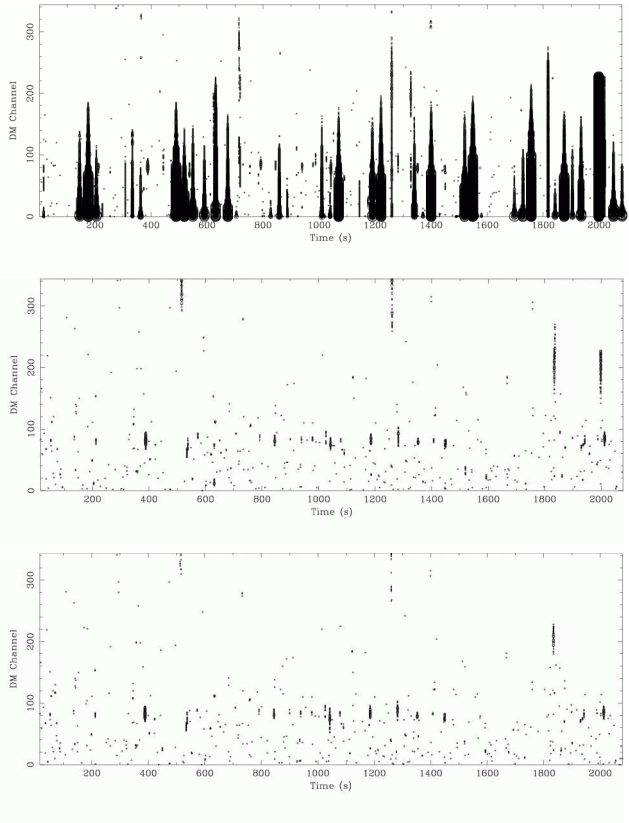


**Figure 7.** Single-pulse search diagnostic plots of a 35-minute observation of the erratic pulsar PSR B1735-32. Top: using standard search method without zero-DM filter; Broadband terrestrial interference causes the large stripes across a wide range of DM. Middle: After using zero-DM filter, most RFI streaks have been removed with single pulses from the pulsar now much more visible (at DM channel  $\approx 82$ ). Bottom: After using the filter and applying the optimal matched filter. Remnant RFI streaks are further removed and pulses from the pulsar remain.

from PSR B1735-32 at DM channel=82 (DM= $50 \text{ cm}^{-3}\text{pc}$ ), but we can see that the output is contaminated with many RFI streaks making identification of the pulsar difficult. The middle panel shows the corresponding plot with zero-DM filtering applied. The vast majority of the RFI has been removed but the pulsar is still present. Obvious also are a few remnant RFI streaks at high DM which have not been removed by the filtering. Searching the time series with the optimal single-pulse profile,  $w(t)$ , improves things even further by removing the remnant streaks almost completely, as can be seen in the lower panel.

#### 4 DISCOVERY OF FOUR NEW SOURCES

The zero-DM filter has been incorporated into a new re-analysis of the PMPS using acceleration searches (Eatough et al. in prep). So far three new pulsars have been discovered (see Table 1 & Figure 8). Figure 8 shows folded subintegrations and integrated pulse profiles for each of the pulsars in both a standard analysis and after using the zero-DM filter. In all cases impulsive RFI has been removed. Although this demonstrates an improvement in the quality of the folded



**Table 1.** Preliminary properties of the 4 new sources discovered in our re-analyses of the PMPS. The nominal positions quoted are the positions of the centre of the beam in which the source was discovered and have errors of less than 7 arcmin, the radius of the PMPS beam (Manchester et al. 2001).

Name	$\alpha$ (J2000)	$\delta$ (J2000)	Period(s)	DM( $\text{cm}^{-3}\text{pc}$ )
J1724-3549	17:24:43.0	-35:49:18.6	1.4085	550.0
J1539-4835	15:39:18.7	-48:35:14.0	1.2729	136.3
J1819-1711	18:19:50.3	-17:11:48.0	0.3935	400.8
J1835-0115	18:35:13.9	-01:15:17.0	0.0051	98.1

data, the discovery of these sources was primarily aided by either a reduction of RFI features in the fluctuation spectra or because wide spectral filters have not been applied around strong periodic sources of RFI. Of particular interest is PSR J1835–0115, a 5.1-millisecond pulsar in a 6-day orbit around a low mass companion. All three pulsars are now being timed using radio telescopes at either Jodrell Bank or Parkes.

In addition the zero-DM filter is being applied to our re-analysis of the PMPS using single-pulse searches (Keane et al. in prep). Here we present one new source (see Table 1). This source, which has a period of 1.4s, shows single-pulse diagnostic plots which indicate a strong resemblance to the newly-discovered class of Rotating Radio Transients (RRATs) (McLaughlin et al. 2006). Interestingly, this object shows pulses from two parts of the pulse rotation period, separated by about 0.2 sec. We are continuing to monitor this source using the Parkes radio telescope to further constrain the spin period and to obtain a period derivative so it can be compared to the values of period derivative measured for the other RRATs.

## 5 DISCUSSION

Zero-DM filtering reduces the number of spurious candidates detected by pulsar search software - both in standard periodicity searches and in single-pulse searches. A major advantage of zero-DM filtering is that it eliminates the need to apply arbitrary cleaning techniques to pulsar search data. One commonly-used technique is that of clipping the multi-channel data based upon spikes in the DM=0 time series (e.g. Hobbs et al 2004). For 1-bit sampled filterbank data like that in the PMPS, with  $n$  channels, the time samples should have a mean of  $n/2$  and a standard deviation of  $\sqrt{n}/2$  (e.g. Lorimer & Kramer 2005). Typical clipping algorithms set each of the  $n$  channels to alternate zeros and ones if the time sample differs from the mean by more than three standard deviations. Clipping could pose a threat to intense burst-like dispersed signals that are strong enough to be detected in the low-DM trials of a pulsar search. It is precisely these type of transient events which may reveal exciting new astrophysical phenomena (Lorimer et al. 2007). Since zero-DM filtering relies on the undispersed nature of RFI, rather than its sheer strength, such signals will not be removed.

The primary RFI excision technique for pulsar periodicity searches up until now has been frequency domain ‘zapping’. This method requires the identification of common

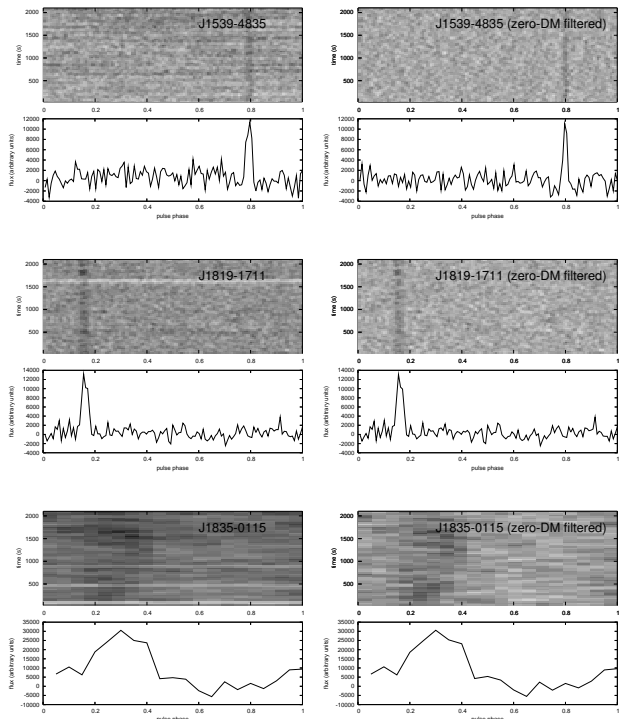


**Figure 8.** Folded subintegrations and integrated pulse profiles for three of the pulsars discovered. For each pulsar we show the standard analysis on the left and the zero-DM filtered data on the right.

signals in the fluctuation spectra from independent observations at different positions on the sky. Such signals likely have a local terrestrial origin and enter the receiver system through the far-out sidelobes of the telescope beam. Once the RFI signals have been identified their harmonic sequence is removed from the fluctuation spectrum. Typical spectral zapping routines can remove a few percent of the fluctuation spectrum giving a small chance that a coincident pulsar frequency or its harmonics could be removed. The zero-DM filtering process presents a more natural way of removing such RFI signals without the dangers inherent to zapping.

Although effective at removing RFI in our analyses of the PMPS, we now note a number of limitations and practicalities of the zero-DM filter. Firstly the technique will not benefit high-frequency, or small bandwidth pulsar searches because in this case even signals from celestial sources will not be highly dispersed. For example, the dispersive delay across the entire 576-MHz bandwidth in the Parkes methanol multi-beam pulsar survey at 6.3 GHz is less than 2 ms for a source with DM=100  $\text{cm}^{-3}\text{pc}$  (e.g. O’Brien et al. 2008.). In this case the zero-DM filter would have a low-frequency cutoff around 230 Hz making detection of all but millisecond pulsars impossible.

In single-pulse searches, impulsive RFI signals can occasionally be strong enough to persist even after zero-DM filtering. The remnant RFI streaks appear as high signal-to-noise features at non-zero DM. However such remnant RFI streaks will not have the expected drop off in signal-to-noise ratio as a function of trial DM, nor will they appear dispersed according to Equation 1 like a true celestial source. They are also likely to appear in multiple beams of a multi-

beam receiver. Each of these additional properties can be used to identify such spurious signals.

An assumption made in the analysis of the implementation of the zero-DM filter is that of a linear dispersion slope when the true slope is in fact quadratic. A complete description of the dispersion slope increases the difficulty of implementing the algorithm, with little benefit. The effects of this assumption manifest themselves in phase-folded pulse profiles which have asymmetric dips as shown in Figure 5 for PSR J1842+0257, unlike the symmetric dips we have considered in Figure 1.

Future pulsar surveys will be performed with higher time and frequency resolution<sup>2</sup>. Fast dedispersion codes are being developed to cope with the large volume of data that will be produced (Bailes, private communication). These dedispersion algorithms operate on 1-bit or 2-bit data before the samples have been unpacked as floating point numbers. In these algorithms, calculation of the mean and subsequent subtraction from each frequency channel sample as in Equation 2 may not be possible at the pre-dedispersion stage.

The factor of two increase in the number of computations imposed by re-application of the zero-DM filter after every dispersion trial might not be practical in searches where large numbers of Fast Fourier Transformations are performed, viz. searches for highly accelerated binary pulsars (e.g. Eatough et al. in prep). Another practical consideration is for data sampled with a larger number of bits, i.e. a large dynamic range. In this scenario any RFI with intensity structure across the band may ‘leak’ through the zero-DM filter.

We have implemented the zero-DM filter in the *Sigproc-4.2* pulsar analysis software suite and are currently applying the process in a re-analysis of the PMPS in both acceleration searches (Eatough et al. in prep) and single-pulse searches (Keane et al. in prep).

## ACKNOWLEDGEMENTS

This research was partly funded by grants from the Science & Technology Facilities Council. Evan Keane acknowledges the support of a Marie-Curie EST Fellowship with the FP6 Network “ESTRELA” under contract number MEST-CT-2005-19669. The Australia Telescope is funded by the Commonwealth of Australia for operation as a National Facility managed by the CSIRO. We would like to thank M. Kramer, B. Stappers, and C. Jordan for useful discussions and manuscript reading. We also acknowledge A. Forti and The University of Manchester Particle Physics group for use of the Tier2 computing facility<sup>3</sup>.

## REFERENCES

Hobbs G., Faulkner A., Stairs I. H., Camilo F., Manchester R. N., Lyne A. G., Kramer M., D’Amico N., Kaspi V. M., Possenti A., McLaughlin M. A., Lorimer D. R., Burgay M., Joshi B. C., Crawford F., 2004, MNRAS, 352, 1439

Lorimer D. R., Bailes M., McLaughlin M. A., Narkevic D. J., Crawford F., 2007, Science, 318, 777

Lorimer D. R., Kramer M., 2005, Handbook of Pulsar Astronomy. Cambridge University Press

Lyne A. G., Smith F. G., 2006, Pulsar Astronomy, 3rd ed.. Cambridge University Press, Cambridge

Manchester R. N., Lyne A. G., Camilo F., Bell J. F., Kaspi V. M., D’Amico N., McKay N. P. F., Crawford F., Stairs I. H., Possenti A., Morris D. J., Sheppard D. C., 2001, MNRAS, 328, 17

McLaughlin M. A., Lyne A. G., Lorimer D. R., Kramer M., Faulkner A. J., Manchester R. N., Cordes J. M., Camilo F., Possenti A., Stairs I. H., Hobbs G., D’Amico N., Burgay M., O’Brien J. T., 2006, Nature, 439, 817

O’Brien J. T., Johnston S., Kramer M., Lyne A. G., Bailes M., Possenti A., Burgay M., Lorimer D. R., McLaughlin M. A., Hobbs G., Parent D., Guillemot L., 2008, MNRAS, 388, L1

<sup>2</sup> <http://astronomy.swin.edu.au/pulsar/?topic=hlsurvey>

<sup>3</sup> <http://www.hep.manchester.ac.uk/computing/tier2>